

An experimental investigation of the oscillating lift and drag of a circular cylinder shedding turbulent vortices

By J. H. GERRARD

Department of the Mechanics of Fluids, Manchester University

(Received 13 March 1961)

The oscillating lift and drag on circular cylinders are determined from measurements of the fluctuating pressure on the cylinder surface in the range of Reynolds number from 4×10^3 to just above 10^5 .

The magnitude of the r.m.s. lift coefficient has a maximum of about 0.8 at a Reynolds number of 7×10^4 and falls to about 0.01 at a Reynolds number of 4×10^3 . The fluctuating component of the drag was determined for Reynolds numbers greater than 2×10^4 and was found to be an order of magnitude smaller than the lift.

1. Introduction

In the last 30 years more than sixty papers have been published on subjects closely related to vortex shedding from circular cylinders in subsonic flow. Apart from the fact that the phenomenon is far from completely understood, this continued interest in a classical subject is partly due to improved instrumentation, making possible the measurement of the intensity of fluctuating quantities. Recently renewed interest has followed on Lighthill's publications (1952, 1954) on aerodynamic sound. Fifteen of the papers mentioned above are concerned with the acoustical concomitant of vortex shedding known as Aeolian tones. Lighthill's theory was applied to the problem of Aeolian tones by Curle (1955) and Phillips (1956). They show that in the presence of a rigid body the sound field is dominated at low Mach numbers by dipole radiation attributable to the fluctuating pressure at the surface of the body.

In the case of a circular cylinder shedding vortices, the main component of the acoustic radiation is a single dipole field which results from a surface pressure distribution, equivalent to that which would be produced by a fluctuating circulation round the cylinder in inviscid flow: the integral of this surface pressure distribution is the fluctuating lift. A second but smaller component is also produced as vortices of alternate sign grow and pass downstream; it has twice the frequency of the fluctuating lift and arises from the pressure distribution responsible for the fluctuating drag.

It can be shown, by applying dimensional analysis to the fundamental equation of Curle and Phillips, that the acoustic intensity at large distances

from a cylinder of finite length in the plane of symmetry bisecting the cylinder at right angles, is given by

$$I \propto \frac{\rho \sin^2 \theta}{a^3 r^2} U^6 S^2 \bar{l}^2 \overline{C_L^2}. \quad (1)$$

Bars denote means with respect to time, and

ρ	= free stream density,
a	= free stream speed of sound,
r, θ	= polar co-ordinates, $\theta = 0$ being the upstream direction,
U	= free stream velocity,
$S = Nd/U$	= Strouhal number,
d	= cylinder diameter,
N	= vortex shedding frequency,
l	= a representative length of the cylinder which will depend on the phase variation along the cylinder length
C_L	= lift coefficient = (lift per unit length)/ $\frac{1}{2}\rho U^2 d$.

Equation (1) relates the intensity of Aeolian tones to the parameters of the flow. In order to compare experimental investigations of the radiated sound with this equation, resort must be had to experimental evidence or to assumptions concerning the parameters S , l and C_L . The Strouhal number, S , is a well-established function of Reynolds number for the whole of the range (35 to 10^5) within which vortices are shed; see, for example, Cometta (1957), Gerrard (1955). The value of S , in fact, differs by less than 10% from the value 0.20 for Reynolds numbers greater than about 300. This parameter will produce no spectacular variation in equation (1).

The purpose of the present investigations is to determine the fluctuating lift coefficient as a function of Reynolds number. The spanwise correlation of the oscillations which determine the effective length l will not be discussed here.

2. Experimental apparatus

2.1. The wind tunnel

A return-circuit wind tunnel of 20 in. \times 20 in. working section was used for these experiments. The tunnel was designed to have a low turbulence level. The intensity of the axial component of turbulence was less than 0.30% at distances greater than 3 in. from the walls. The thickness of the boundary layer on the tunnel walls at the model position was $1\frac{1}{2}$ in.

The models were mounted in the centre of the 10 ft. long working section; they spanned the tunnel vertically mid-way between the side walls. The static pressure varied from floor to roof at the model position by about $\frac{3}{4}$ % of the kinetic pressure. The working section static pressure was atmospheric and made constant along the working section in the absence of the model by adjustment of the position of the roof.

Corrections to the velocity of the air flow to account for the effect of the tunnel walls were investigated in the manner described by Pankhurst & Holder (1952).

These included a consideration of the lift correction. The only significant corrections were found to be those due to the blockage of the flow by the cylinder and its wake.

2.2. Models

The circular-cylinder models were metal tubes and had outside diameters of 3, $1\frac{1}{2}$, 1, $\frac{9}{16}$ and $\frac{1}{4}$ in., there being two models of 1 in. diameter. The pressure pick-ups were mounted midway along the length of the cylinders. In the case of the cylinders of smaller diameter, electrical connexions were taken along the axis of the cylinder from the pick-up to a pre-amplifier outside the tunnel. The

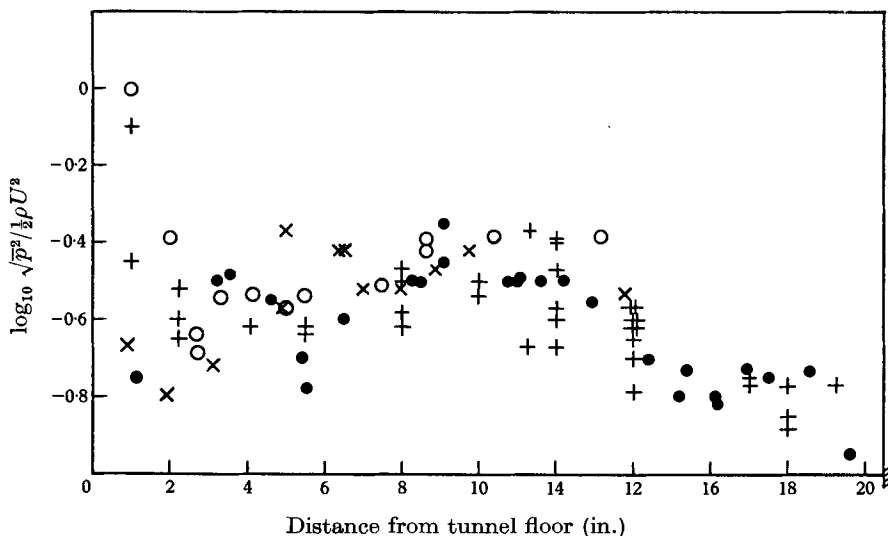


FIGURE 1. Spanwise variation of the fundamental component of oscillating pressure 120° from the front of the cylinder ($\theta = 0^\circ$) on 1-in. diameter cylinders.

	Tunnel	Model	$\log_{10} R$
●	Low turbulence	{No. 1	4.46
+		{No. 2	4.46
×	Open circuit	{No. 2	4.36
○		{No. 2	4.59

3 in., $1\frac{1}{2}$ in., and one of the 1 in. diameter models had the preamplifier mounted inside the model close to the pressure pick-up. This was found not to increase the true to spurious signal ratio because vibration of the leads and of the pre-amplifier produced roughly equal effects.

Various types of cylinder mounting were tried in an attempt to reduce cylinder vibration to a minimum. Rigid contact with the tunnel floor and roof increased the vibrations since these vibrated at the vortex shedding frequency under the driving force of the wake. No appreciable effect on the cylinder surface pressure at the centre of the tunnel was observed when the mounting was changed. Resonance vibration was, of course, avoided but the conclusion reached after many unsuccessful attempts to eliminate vibration was that it is virtually impossible to produce a rigid cylinder.

2.3. Pressure pick-up position

The sensitive area of the pressure pick-up was flush with the cylinder surface. Measurements at various positions round the circumference of the model were made by rotating the cylinder. The 3 in. diameter cylinder carried two pressure pick-ups separated by 1 in. in the spanwise direction: these could be rotated independently to determine the phase distribution of the fluctuating pressure round the circumference.

The pressure pick-up was generally at the centre of the tunnel. Only with the 1 in. models was a spanwise traverse made. The results are shown in figure 1. This graph also illustrates the repeatability of the results. The measurements in the low turbulence tunnel were made with two models (both 1 in. diameter) and with different mountings. Some measurements were made in an open-circuit wind tunnel of the same working-section cross-section. This had a free stream turbulence intensity of 7–10 %, some 200 times greater. At the Reynolds numbers investigated this increased turbulence had no apparent effect.

Despite the large scatter (the greatest spread excluding points close to the floor is about 6db), there appears to be some systematic variation across the span. There is little variation over the centre third of the model length and end-effects, if such they be, have not been investigated. In what follows all the measurements were obtained at the centre of the low-turbulence tunnel.

2.4. The pressure pick-ups

The pressure pick-ups used are essentially condenser microphones. Piezo-electric gauges were tried but proved in this application to be more sensitive to vibration than to the pressure on their surface. The pressure pick-ups are the only part of the instrumentation which is in any way novel and they will therefore be described fully. They are easily made and fit flush with the cylinder surface. A cross-section of what may be called the standard pressure gauge fitted in most models is shown in figure 2. Those in the 3 and $\frac{1}{4}$ in. diameter models are differently mounted but the same in principle.

The design is based on the 'condenser microphone with solid dielectric' described by Kuhl *et al.* (1954). In essence the microphone consists of an insulated back-plate and a metal-foil front plate separated by a dielectric foil. The microphone functions by the applied pressure compressing the occluded air between the solid dielectric and the back-plate; the signal is produced by the fluctuations in capacity.

Here the back-plate is simply a 4 BA cheesehead screw with the head turned down beyond the slot and then grooved. This is held in a $\frac{1}{2}$ in. Perspex cylinder which fits across the inside of the model as shown in the figure, and the part protruding is machined off. The signal lead (a metal rod) is held against the back-plate screw. The front plate of the condenser microphone is a 0.001 in. silver foil which is soldered at one point to the cylinder surface which is the earth connexion. The solid dielectric consists of a thin piece of paper (typing copy paper) soaked in a silicone preparation and dried. Without the silicone treatment the microphone self-noise is high. The paper and silver foil are

smoothed in place and pressed hard onto the back-plate and secured with a little silicone varnish.

The sensitivity of such an instrument with a circular sensitive area of $\frac{1}{4}$ in. diameter is about -110 db on 1 V/dyne cm^{-2} or $3.16 \mu\text{V/dyne cm}^{-2}$, and this remains constant to within a few decibels in 12 months; the short-term stability is also good. When the mean ambient pressure changes, the calibration changes if there is no leak between the atmosphere and the occluded air within the microphone. No leakage was included in these pressure gauges and so a small error is introduced. The mean pressure on the cylindrical-model surface differed from atmospheric between the limits of $+7$ cm of water and -20 cm of water according to position at the highest tunnel speed. Calibration of the microphones with varying ambient pressure showed that for this range of ambient

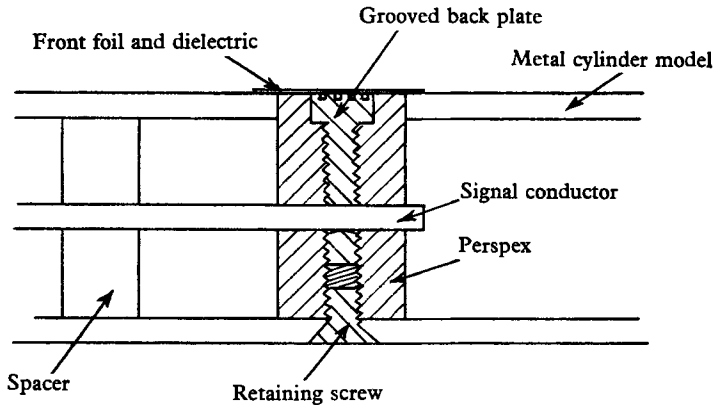


FIGURE 2. Pressure pick-up.

pressure the sensitivity varied by less than 1 db from -110 db on 1 V/dyne cm^{-2} and so no effort has been made to correct for the variation or to construct a leak in the pressure gauge.

The pressure pick-ups covered a large angular range on the cylinder surface. It was fortunate that in this application the large size of the sensitive area was relatively unimportant. The fluctuating pressure intensity only varies rapidly with position at the front and rear of the cylinder where it contributes little to the lift. Pressure distributions were measured with the larger models. With models of diameter less than 1 in. measurements were made in the region $90^\circ < \theta < 150^\circ$, in which the intensity is almost independent of the angle θ , where θ is the angle subtended at the axis, and is measured from the front of the cylinder. To determine the lift it was assumed that the angular distribution of pressure was the same on the smaller diameter cylinders as it was on the larger.

2.5. Measuring apparatus

A block diagram of the measuring and calibration apparatus is shown in figure 3 which needs little explanation. The pressure pick-up was calibrated by comparison with a B and K type 4111 condenser microphone by enclosing both in a closed coupler driven by a loudspeaker. This was done during each series of

measurements whilst the model was in the wind tunnel. The electronic apparatus following the pre-amplifier was also calibrated by inserting a standard signal at the relevant frequencies during each set of measurements.

Initially the wave analyser was a set of $\frac{1}{3}$ -octave filters centred at fixed frequencies; later, a Muirhead D-788-A low-frequency analyser was used.

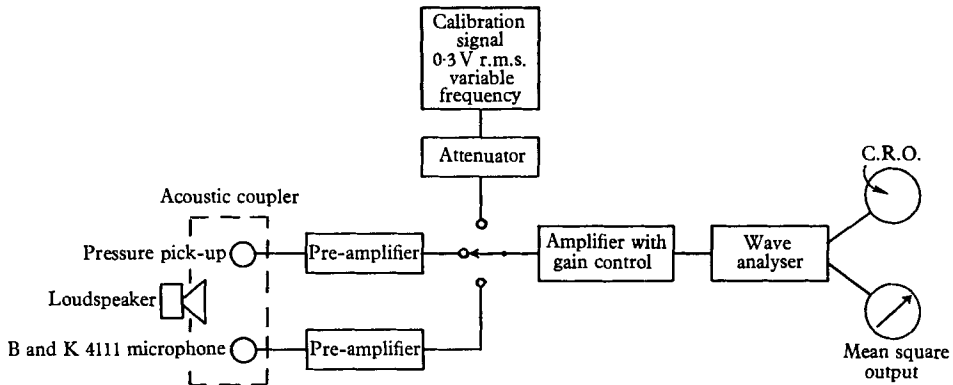


FIGURE 3. Measuring and calibration apparatus.

3. Experimental results

Extensive measurements have only been made with models of diameters 1 and 3 in. The other models were used to extend the Reynolds number range of the measurements. The appearance of the signal from the pressure pick-up was similar in all cases: frequency and intensity varied with position on the cylinder and with the flow parameters, but in all cases the signal had the appearance of a narrow band of noise, that is, a pure-tone amplitude modulated with lower frequencies. Some examples of the appearance of the traces on the cathode-ray tube are shown in figure 4. The modulation of the signal appears random, as would be expected if the governing mechanism depended on the details of a flow structure which was turbulent.

3.1. Frequency

The signal is close enough to a pure tone for frequencies to be determined by means of a Lissajous figure. It is simple, however, to use a narrow band filter of variable frequency. In all cases the latter method was used. This measurement served as a check that the cylinder was not executing some strong vibration. When this occurred the results were discarded. Some of the frequency measurements are plotted in figure 5, which shows agreement with previous measurements. The symbols on figure 5 refer to the same cylinder diameters as those on figure 10.

3.2. Spectra

The spectrum of the pressure fluctuations varied with position round the cylinder. It was rich in the second harmonic (the frequency of the fluctuating drag) at the rear of the cylinder ($\theta = 180^\circ$), but almost lacking in harmonics at

angles θ less than 120° . In general, the width of the spectrum increased with increased velocity. Three observed spectra are shown in figure 6. As velocity increases there appears to be a relative increase in the signal at frequencies above the fundamental. Only at high fundamental frequencies does the signal below the fundamental frequency increase with velocity. The trend, however, is a broadening of the spectra as velocity is increased. If the broadening is due

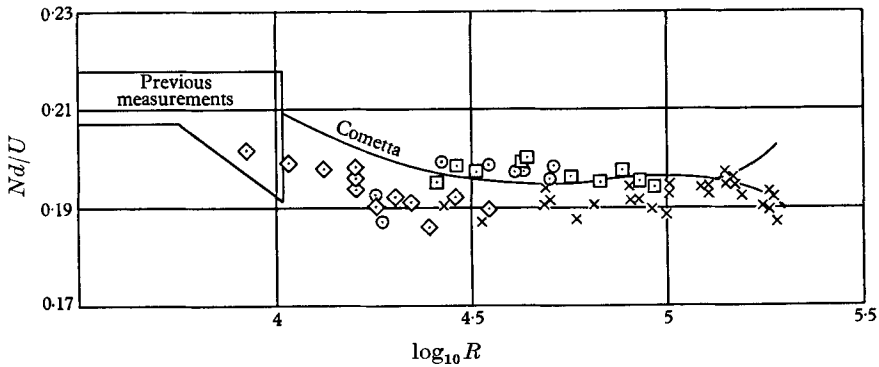


FIGURE 5. Strouhal number.

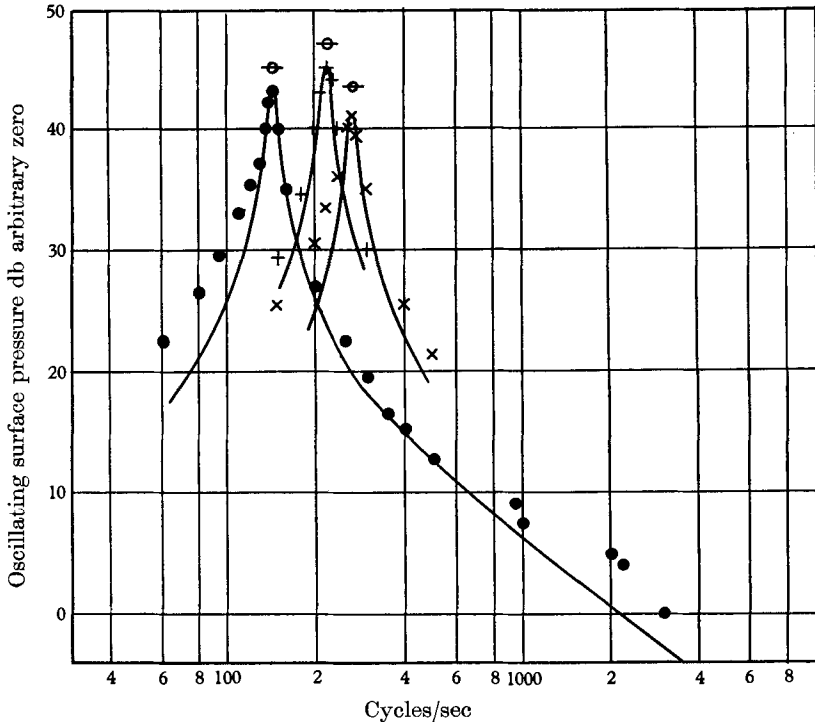


FIGURE 6. The increase of spectral width with increase of free-stream velocity; cylinder diameter 1 in., measurements at the surface 90° from the front of the cylinder. ●, 1660 cm sec^{-1} ; +, 2670 cm sec^{-1} ; ×, 3230 cm sec^{-1} ; ⊖, level measured with no filter; —, curve for pure tone signal.

to turbulent fluctuations we can expect the spectra to be broader at higher Reynolds numbers.

The reduced intensity at the higher velocity was often observed: two different readings appear to be possible at the high velocities as can be seen in figure 10. This behaviour is unexplained. It is perhaps worth noting in connexion with these spectra that some measurements were made up to 16.5 kc/sec on signals such as those in figure 6. The level fell off monotonically as it is shown doing in figure 6 and no peaks were observed in the spectrum at higher frequencies. This is contrary to the findings of Shaw (1951).

3.3. Angular distribution of phase

The 3 in. model was equipped with two pressure gauges separated by 1 in. in the spanwise direction; these could be rotated independently. Measurements were thus taken of the phase difference between the fundamental-frequency

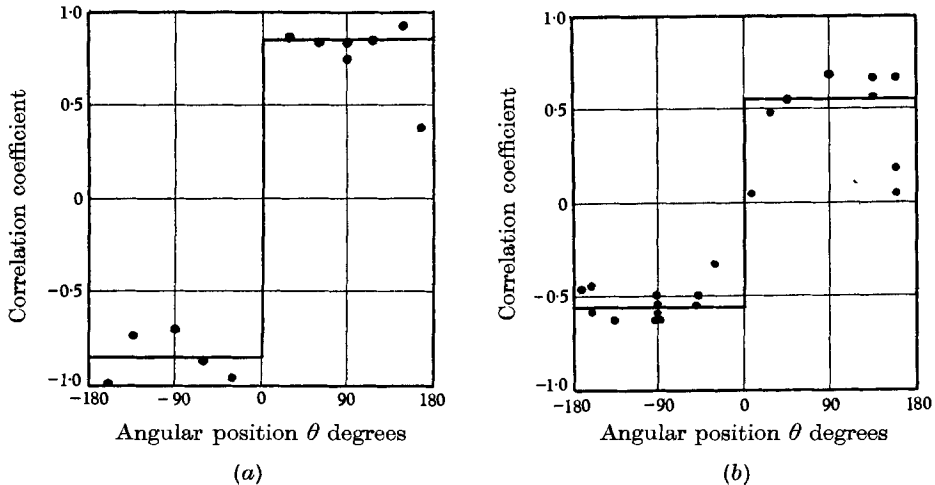


FIGURE 7. Angular distribution of surface-pressure correlation-coefficient on the 3 in. diameter model. (a) Reynolds number = 114,000. (b) Reynolds number = 85,400.

signals of the two gauges, one at a fixed position at $\theta = 90^\circ$, the other in positions from $\theta = -180^\circ$ to 180° . The results are shown in figure 7. They indicate essentially that the pressure is in phase over one side of the model and 180° out of phase with that on the other side. It is seen, however, that the correlation has dropped significantly from unity even in the $\frac{1}{3}$ diameter separation of the gauges. Lack of correlation may be due either to phase change of the fundamental frequency or to the change in phase of the fluctuations in the amplitude along the span. Spanwise-variation investigations have been deferred to later and will involve further experimental work. Little error will be introduced by assuming that the signal is in phase from 0 to 180° and of opposite phase on the other side. Though the transition may not occur rapidly at $\theta = 0$ and 180° the signal level is small in these regions.

3.4. Angular distribution of intensity

The distribution of oscillating pressure round the cylinder is shown in figure 8 for the fundamental-frequency component. It is seen not to vary significantly with Reynolds number. Comparison is made with the experimental results of McGregor (1957) obtained with a $1\frac{1}{8}$ in. cylinder. The values plotted are uncorrected for the size of the sensitive area of the pressure gauge.

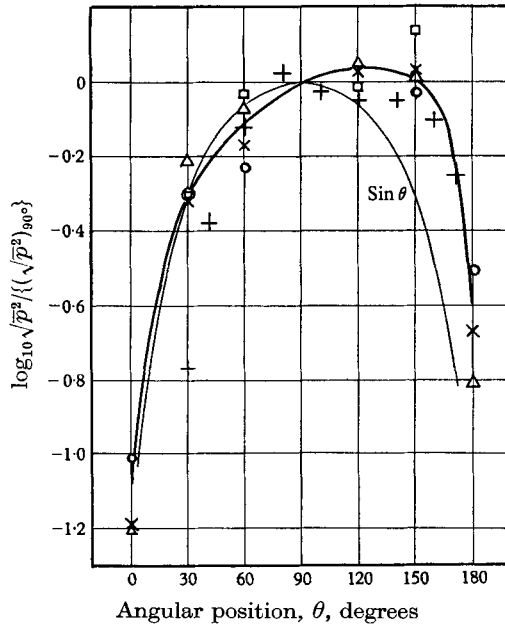


FIGURE 8. Angular distribution of intensity of surface pressure at the fundamental frequency. $\log_{10} R$: \square , 4.1; \triangle , 4.3; \times , 4.8; \circ , 5.2; $+$, McGregor 4.64.

The second harmonic distribution is shown in figure 9 for several velocities and three cylinder diameters. McGregor's values are again included. The measurement of second harmonic intensity is difficult because it is so much smaller than the fundamental, except at $\theta = 180^\circ$. The measurements fall reasonably on one curve nevertheless.

Measurements with the cylinders of diameters other than 1–3 in. inclusive were confined almost entirely to the fundamental frequency in the angular range 90 – 150° . It was assumed that the angular distribution of intensity was the same in all cases. The fundamental-fluctuating pressure coefficient is plotted as a function of Reynolds number in figure 10 for several positions on the cylinders. At high velocities there appear to be two intensities possible in some cases. These are joined by vertical lines on figure 10. No explanation is offered for this behaviour.

3.5. The lift and drag

The fact that the pressure is in phase on one side of the cylinder and out of phase with that on the other side allows us to calculate the lift on the cylinder by integrating the pressure. The assumption of no change in the angular dis-

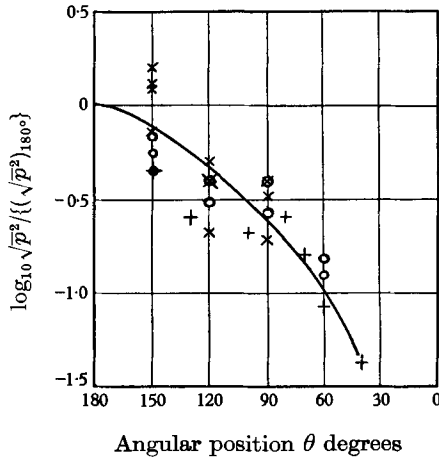


FIGURE 9. Angular distribution of intensity of surface pressure at the second harmonic frequency. \odot , 1 in. diam. cylinder; \times , 3 in. diam. cylinder; $+$, McGregor, $1\frac{1}{2}$ in. diam.

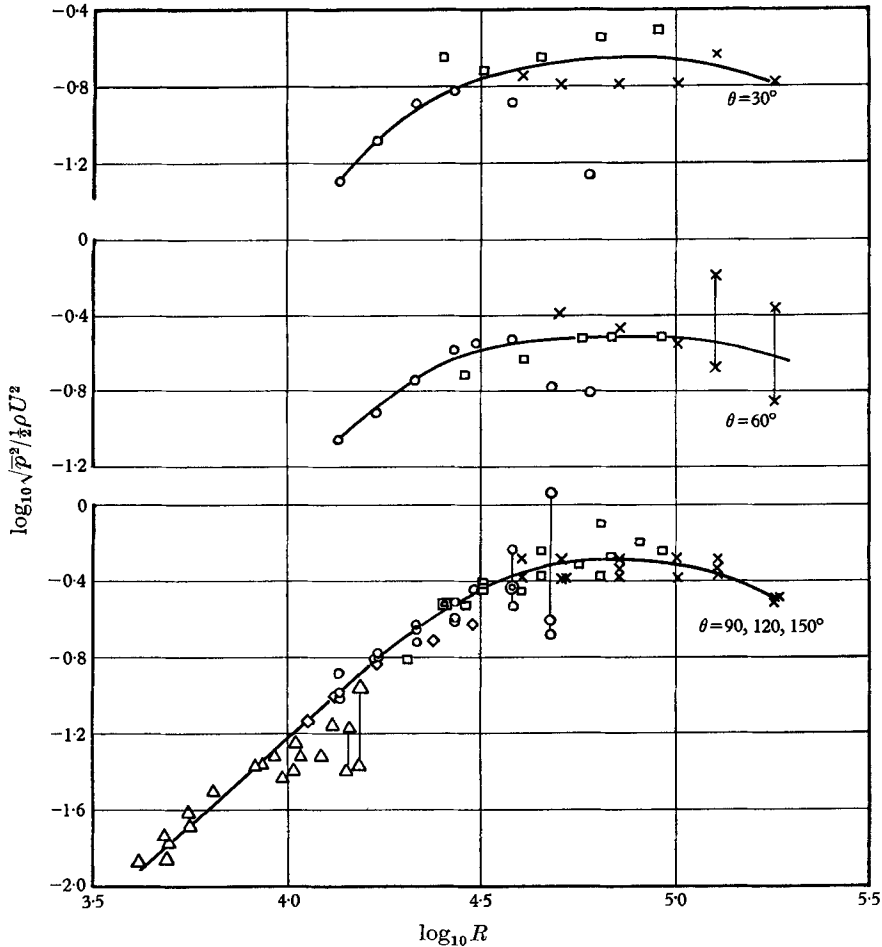


FIGURE 10. Fundamental frequency oscillating pressure coefficient. Cylinder diameter in in.: \diamond , 0.56; \circ , 1; \square , 1.5; \times , 3; \triangle , 0.25.

tribution of phase or intensity down to the lowest Reynolds numbers investigated seems unlikely to produce a large error in the lift. There appears to be no reason why the phase distribution should change with Reynolds number: this belief is substantiated by the predicted dipole nature of the radiated sound field (Curle 1955) which has also been observed at lower Reynolds numbers (Gerrard 1955). The intensity distribution may depend upon the Reynolds number for it was only measured in that range in which the r.m.s. lift does not vary. Even if the angular distribution of intensity changes to a $\sin \theta$ curve, the resulting change in the lift is only about 10 %.

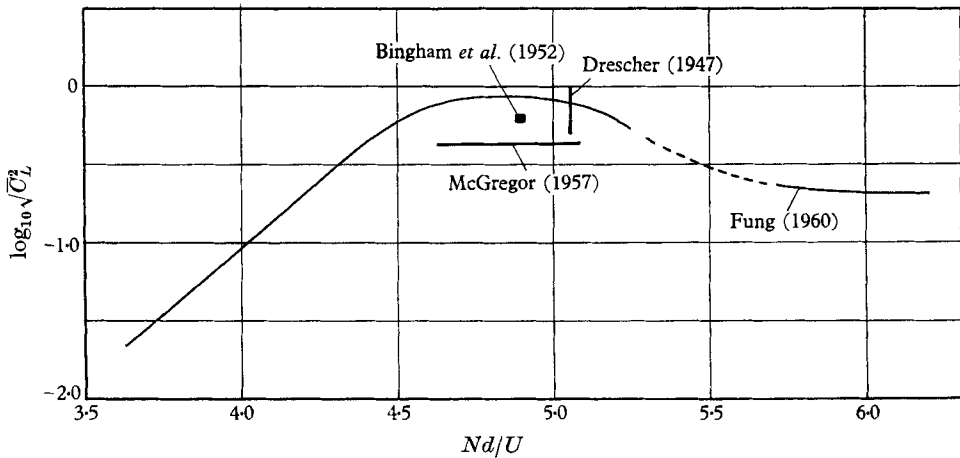


FIGURE 11. Root-mean-square lift coefficient.

The calculated lift coefficient is plotted in figure 11 and compared with the measurements of other workers. The agreement is seen to be fairly good. The measurements of Bingham, Weimer & Griffith (1952) were obtained in a shock tube during the first few cycles of oscillation of the lift. Drescher's (1947) measurements were in water at a frequency low enough to follow with a manometer. Fung's (1960) measurements refer to the more random fluctuations beyond the critical Reynolds number and were obtained directly as the lift force on a section of the cylinder about two diameters in length. The cylinder was 12 in. diameter and 72 in. long. McGregor's (1957) experimental arrangement was similar to that of the author. His measurements lie below those reported here by about 6 db, which is larger than the errors believed to be present by either author. More recent measurements by Humphreys (1960) at Reynolds numbers above 4×10^4 agree with both those of McGregor and those of the author. Humphreys's two sets of measurements were obtained by altering the geometry at the cylinder-wall junction. We have observed an effect of small disturbances at the cylinder ends (Gerrard 1958): the pressure at the cylinder centre was found to be altered by 1 db (10 % of p^2) by small alterations of end geometry. The 6 db change reported by Humphreys may be attributable to the fact that his measurements are an average over the whole cylinder and therefore include any changes of spanwise distribution caused by the change in end conditions.

The fluctuating component of the drag may be determined from the second harmonic pressure intensities if we make an assumption about the phase. The most logical assumption is that the second harmonic pressure is of the same phase over all the cylinder. The resulting drag coefficients are between 10 and 13 times less than the lift coefficients and are plotted in figure 12. They are seen to agree with McGregor's values which are included for comparison. There is a large scatter in the measurements which is attributed to the difficulty of accurate measurements of the second harmonic in the presence of the much larger fundamental component.

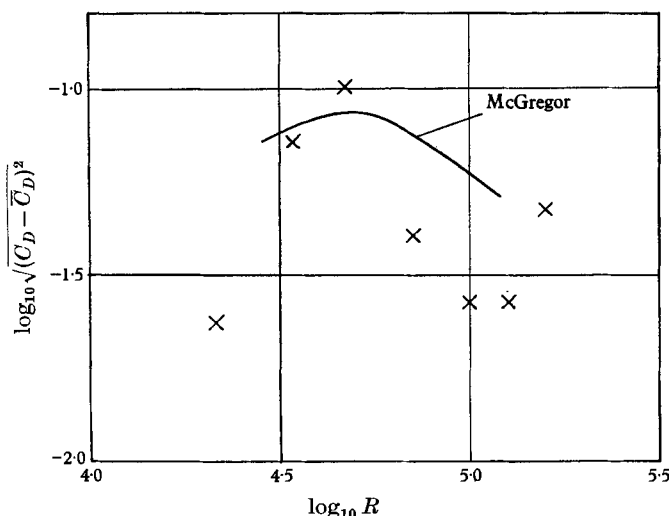


FIGURE 12. Root-mean-square oscillating component of the drag.

4. Discussion

The work reported in this paper extends the range of measured lift coefficient to lower Reynolds numbers than other workers achieved. The result of this extension of the Reynolds number range is the observed large change in lift coefficient, by nearly two orders of magnitude, as the Reynolds number changes from 4000 to 20,000. In this range the experiments indicate a power law relation between lift coefficient and Reynolds number, viz. $\sqrt{\bar{C}_L^2} \propto R^{1.7}$. From equation (1) we expect the intensity of the sound radiated by the flow past the cylinder to vary with Reynolds number like $\bar{C}_L^2 \bar{l}^2$. In the Reynolds number range from 1500 to 10,000 the measured sound intensity was found to vary like R^3 by Gerrard (1955). The implication is that the effective length, l , of the cylinder varies little with Reynolds number in this range since almost all the Reynolds number variation of the sound intensity can be accounted for by that of the lift coefficient. Our intention is to investigate the spanwise structure of the flow over this Reynolds number range. The measurement of the oscillating component of the drag is difficult at Reynolds numbers less than 10^4 since large pressures are expected only on small diameter cylinders. Whether or not the oscillating drag coefficient falls off below this Reynolds number is unknown.

REFERENCES

- BINGHAM, H. H., WEIMER, D. K. & GRIFFITH, W. 1952 The cylinder and semicylinder in subsonic flow. *Princeton Univ. Tech. Rep.* II-13.
- COMETTA, C. 1957 An investigation of the unsteady flow pattern in the wake of cylinders and spheres using a hot-wire probe. *Brown Univ. Tech. Rep.* WT-21.
- CURLE, N. 1955. The influence of solid boundaries on aerodynamic sound. *Proc. Roy. Soc. A*, **231**, 505.
- DRESCHER, H. 1947 *Model Testing Techniques. II.* 6. *Measurement of unsteady pressure.* AVA monographs D2. (Translation: *Aero. Res. Council. Rep.* no. 11,391.)
- FUNG, Y. C. 1960 Fluctuating lift and drag acting on a cylinder in a flow at supercritical Reynolds numbers. *J. Aerospace Sci.* **27**, 801.
- GERRARD, J. H. 1955 Measurements of the sound from circular cylinders in an air stream. *Proc. Phys. Soc. B*, **68**, 453.
- GERRARD, J. H. 1958 Measurements of the fluctuating pressure on the surface of a circular cylinder. Part I. Cylinder of 1 in. diameter. *Aero. Res. Council. Rep.* no. 19,844.
- HUMPHREYS, J. S. 1960 On a circular cylinder in a steady wind at transition Reynolds numbers. *J. Fluid Mech.* **9**, 603.
- KUHL *et al.* 1954 Condenser transmitters and microphones with solid dielectric for airborne ultrasonics. *Acustica*, **4**, 519.
- LIGHTHILL, M. J. 1952 On sound generated aerodynamically. *Proc. Roy. Soc. A*, **211**, 564.
- LIGHTHILL, M. J. 1954 On sound generated aerodynamically. *Proc. Roy. Soc. A*, **222**, 1.
- MCGREGOR, D. M. 1957 An experimental investigation of the oscillating pressures on a circular cylinder in a fluid stream. *Univ. Toronto Inst. Aerophys. Tech. Note* 14.
- PANKHURST, R. C. & HOLDER, D. W. 1952 *Wind Tunnel Technique*, Ch. 18. London: Pitman.
- PHILLIPS, O. M. 1956 The intensity of Aeolian tones. *J. Fluid Mech.* **1**, 607.
- SHAW, R. A. 1951 A preliminary investigation of the acoustic theory of airflow. Low speed wind tunnel tests on an aerofoil and a cylinder. *Aero. Res. Council. Rep.* no. 13,795.

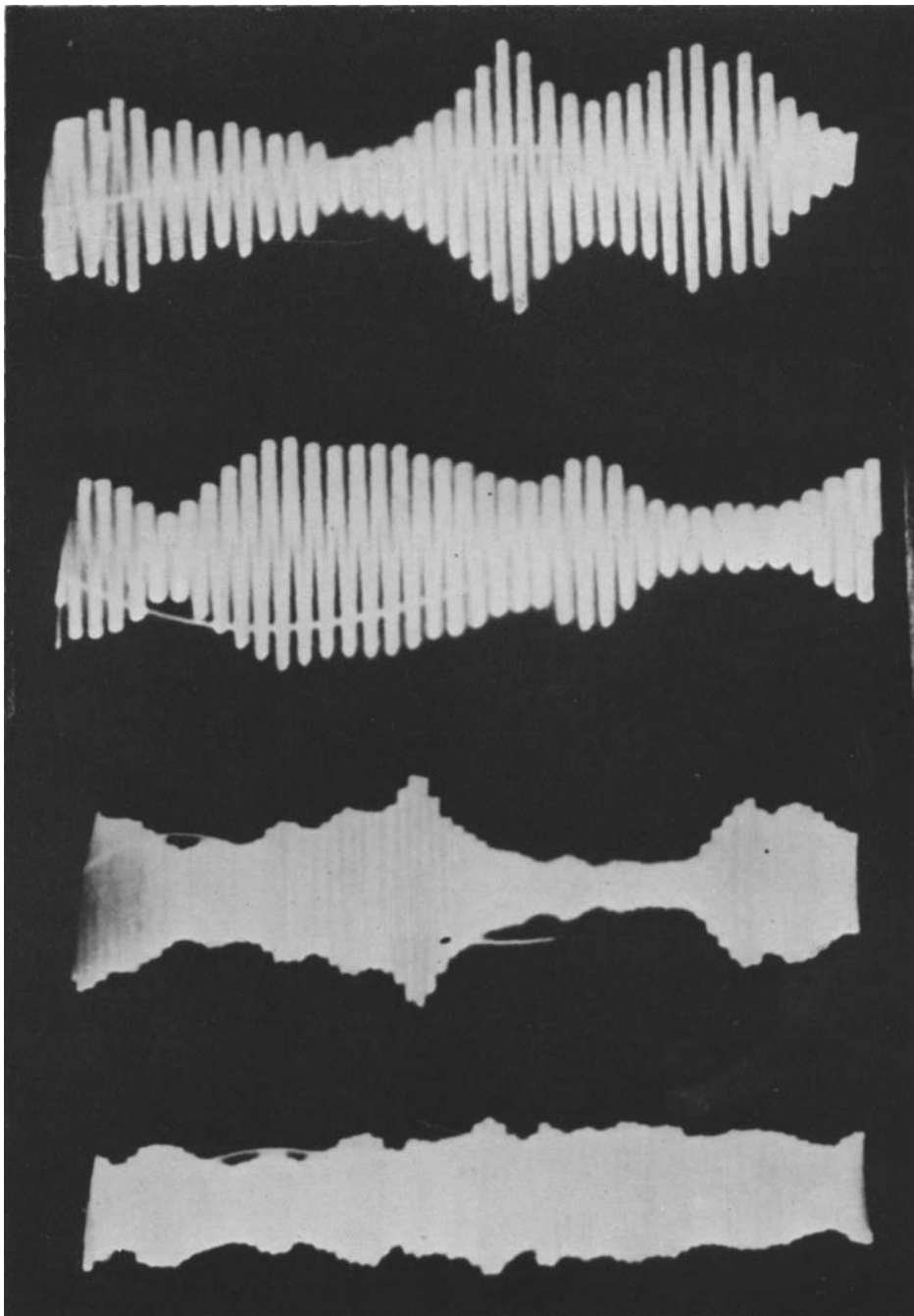


FIGURE 4. Cathode ray oscillograms of surface pressure.